Advanced Materials Research *Online: 2010-06-30*
ISSN: 1662-8985, Vols. 118-120, pp 100-104
doi:10.4028/www.scientific.net/AMR.118-120.100

Measurement on Fracture Roughness Values of the Cast Steel for Chinese Railway Rolling Wagon Bogie Frames

WenDong Shao[1,a] and YongXiang Zhao[2,b,*]

[1]Technical Centre, Qiqihaer Railway Rolling Stock Co., Ltd, Qiqihaer, 161002, China

[2]Institute of Engineering Reliability and Safety, Traction power State key Laboratory, Southwest Jiaotong University, Chengdu 610031, China

[a]shaowendong@126.com; [b]yong_xiang_zhao@163.com; [*]Correspondent

Keywords: Cast steel, Fracture Roughness, Railway, Rolling wagon, Bogie frame

Abstract. Measurement on fracture roughness values is investigated to the grade B cast steel for China railway rolling wagon bogie frames. Due to be limited by production bogie frame geometry, a ductile fracture roughness measuring method is employed for the present study. Experiments reveal that, when crack growth increments are very scattered, the code based measurement of 0.2 mm crack growth increment for gauge ductile fracture roughness may be not reasonable. And a measurement of 90 % maximum ductile fracture roughness should be suggested to be an appropriate measurement. The new suggested 90 % maximum fracture roughness measurement is verified to be effective for the fracture roughness values of the present material.

Introduction

Cast steel is wide used for fabricating bogie frames of railway rolling wagons [1-4]. However, quality of cast steels is highly relative to fabrication technologies e.g. shrink cavity shapes and sizes were greatly affected by the cooling velocity of cast process and the wear resistance of high Cr cast steel was mostly relative to austenite content [5]. Brittleness and grain interface fracture of high Cr and Cr-Mo cast steels can be controlled by moderate contents of aluminum and nitrogen elements plus sustaining temperature out of 900~1200℃ range[6]. Good strength with well roughness and hardness can be obtained to control silence element at around 2.64 % and tempering temperature in a range of 320~360℃ [7]. Yielding velocity of welded hot cracks can be greatly decreased to apply a pre-heat treat to a temperature of 400℃ and to use Ni-Fe alloy as welding flux [8]. In addition, these knowledge and improvements can be not obtained without the experimental researches.

To improve the quality of cast steels and optimize the performances of wagons, series of efforts have been carried out abroad by changing heat treat techniques or adjusting element contents [9-13]. However, up to now, few of experimental researches have been performed on cast steels for Chinese railway rolling wagon bogie frames. This is a great deficiency for improving quality of the cast steels and guaranteeing service safety of the wagon bogie frames [14, 15].

Under foundation of Railway Science and Technology Research and Development Program (Contact No. 2004J013), Southwest Jiaotong University and Qiqihaer Railway Rolling Stock Co., Ltd, carried out together a series of experimental researches to grade B cast steel for making the bogie frames of Chinese railway rolling wagons. Results are introduced in sequence in this conference. Present work investigates the scattered fracture roughness values of material. Purpose is to provide a basis of assessing the critical safety of the bogie frames.

Material, Specimens and Experiments

Material. Present material was machined by Qiqihar Railway Rolling Stock Co., Ltd, for production bogie frames of Chinese railway rolling wagons. By the previous measurements [16], chemical composition is 0.27 C, 0.73 Mn, 0.029 P, 0.01 S, 0.5 Si, 0.16 Al, 1.00 Mo, 0.18 Ca, 0.26 Cr, 0.27 V, 0.25 Ti, 0.34 Ni, 0.33 Cu and the remainder Fe by wt %. Mechanical properties are around 188 GPa

for Young's modulus, 254 MPa 0.2% proof strength, 453 MPa ultimate tensile strength, 26 % elongation, and 45 % reduction of area. The material exhibits lower Young's modulus, higher proportion of yielding to ultimate strengths and reduction of area, and a lower elongation than those of conventional ferrous alloys. Microstructures of the material are consists of sphere ferrites and layer-like pearlites. And point-network like eutectic sulfur compounds, polygonal sphere like Al_2S_3 compounds and hot ties are main casting flaws.

Experiments. Compact tensional (CT) rectangle specimens are used for the present study. By the code ASTM E813-89**,** the effective fracture roughness K_{IC} direct measurement must meet that the specimen geometries (Fig. 1) W, B, a_0, and W-a_0 $\geqslant 0.4(K_{IC}/\sigma_s)^2$ and $0.40 \leq a_0/W \leq 0.6$. Due to limit of structural geometry limit, the present larger possible scale specimens are still too small to meet the code-based requirement. Under this case, a ductile fracture roughness measuring method should be employed, i.e. the ductile resistance J_{IR} curves should be determined firstly and the fracture resistance K_{IR} curve in plan strain state should be obtained through a converting formula. Geometry scales of the specimens for the present study are given in Table 1. All specimens were fatigued on RUMUL 250 kN high frequency fatigue test machine under a continuous decreasing loading mode. Initial loading levels are also given in Table 1. Full tests were carried out under room temperature, air environment, and 0.5 mm.min^{-1} stressing rate. Test P-V and P-Δa curves are exhibited in Fig. 2.

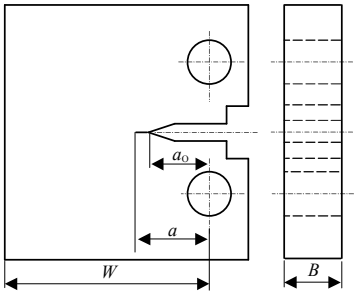

Fig.1 CT specimen for present study

Table 1 Specimen geometries and initial loading levels

Specimen	ΔK_0 (MPam$^{1/2}$)	R	W (mm)	B (mm)	a_0 (mm)
1	7.04	0.1	110.20	50.01	66.29
2	6.90	0.1	110.59	50.00	67.05
3	7.24	0.1	110.10	49.96	67.58
4	7.00	0.1	110.19	50.10	67.21
5	7.00	0.1	110.05	49.97	66.38

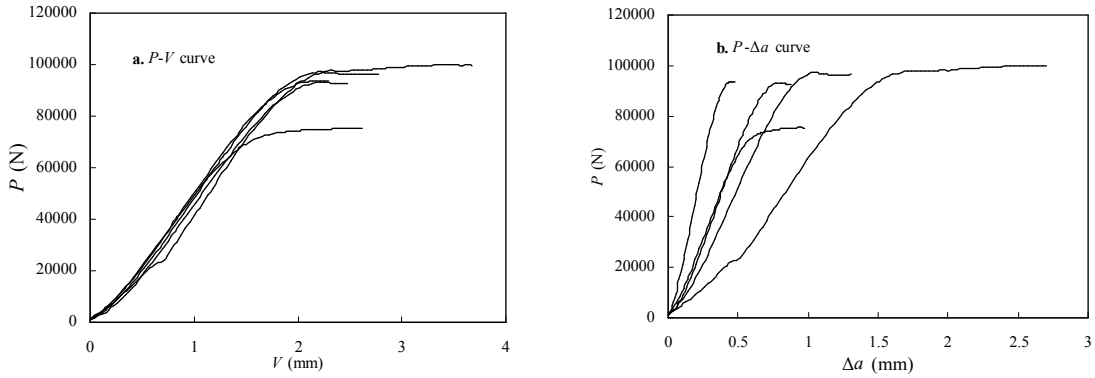

Fig. 2 Test P-V and P-Δa curves for the present material.

Fracture Surface Observations

A SEM graph of a typical fracture surface for material is exhibited in Fig. 3. It revealed that the crack is subjected to growth process and tied transient fracture process. This indicates that the structures of the present material have a ductile critical fracture process. But, from Fig. 3, a most valuable noted issue is that the crack growth increments, i.e. Δa data, appear significant difference.

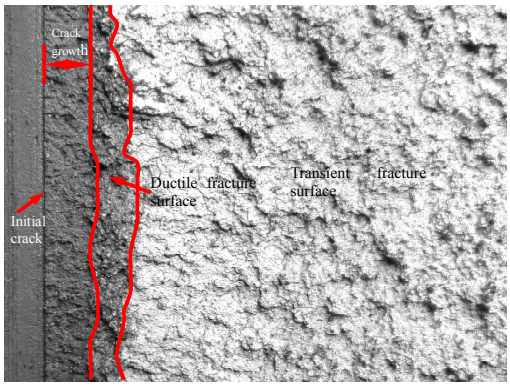

Fig. 3 SEM graph of a typical facture surface for the present material.

Measurement

Resistance Curves. By the test *P*-*V* and *P*-Δ*a* data, ductile resistance J_{IR} curves can be obtained by using the following formulas

$$J_{IR} = \frac{1-\nu^2}{E}\left[\frac{P}{B\sqrt{W}}Y\left(\frac{a}{W}\right)\right]^2 + \frac{2U_p}{B(W-a)};$$
$$Y\left(\frac{a}{W}\right) = \frac{(2+a/W)}{(1-a/W)^{3/2}}\left[0.886 + 4.64\frac{a}{W} - 13.32\left(\frac{a}{W}\right)^2 + 14.72\left(\frac{a}{W}\right)^3 - 5.6\left(\frac{a}{W}\right)^4\right] \quad (1)$$

where *a* is crack length, *v* is poison's ratio; *E* is Young's modulus, U_p is plastic strain energy, *W* and *B* are specimen geometries. When J_{IR} curves are available, the fracture resistance K_{IR} curves in plan strain state can be then determined using the equation below

$$K_{IR} = \sqrt{\frac{E}{1-\nu^2}J_{IR}} \quad (2)$$

By the test *P*-Δ*a* data in Fig. 2, resistance J_{IR}-Δ*a* and K_{IR}-Δ*a* curves are given in Fig. 4.

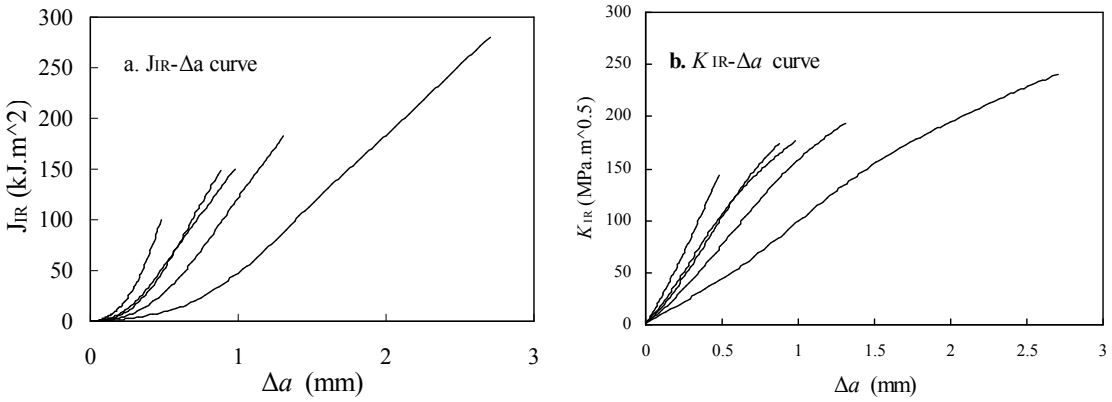

Fig. 4 Resistance J_{IR}-Δ*a* and K_{IR}-Δ*a* curves of the present material.

Appropriate Measurement. By the code ASTM E813-89, an effective measurement must meet the requirements of fracture surface crack morphology, i.e. numbered nine lines representing the crack lengths a_i (*i*=1, 2, …, 9) should be measured with a same interval distance along the crack tip. For the crack length *a*, max $|a_i\text{-}a| \le 0.09B$ when *i*=1 and 9; max $|a_i\text{-}a| \le 0.02B$ when *i*=3, 5, and 7. These parameters for the present tests are given in Table 2. It indicates that the present tests are effective from the crack geometry.

Table 2 Crack geometry parameters max $|a_i\text{-}a|$ for the present tests

Specimen	*a* (mm)	0.02*B* (mm)	Max $\|a_i\text{-}a\|$ (*i*=3,5,7) (mm)	0.09*B* (mm)	Max $\|a_i\text{-}a\|$ (*i*=1,9) (mm)
1	67.17	1.00	0.38	4.51	1.87
2	68.95	1.00	0.56	4.50	3.86
3	68.06	1.00	0.42	4.51	1.51
4	68.19	1.00	0.23	4.51	2.35
5	68.08	1.00	0.68	4.50	3.56

In addition, a gauge ductile fracture roughness, J_{IC}, or deriving the fracture roughness in plan strain state, K_{IC}, should be determined at the 0.2 mm crack growth increment. From the much scattered resistance J_{IR}-Δ*a* and K_{IR}-Δ*a* curves, the measurement by this increment, i.e. the cross points between dotted line and curves in Fig. 5, is not reasonable. Therefore, a measurement of J_{IQ}=90 % J_{Imax} are suggested for deriving the fracture roughness, K_{IQ}, i.e. the cross points between bold solid line and curves in Fig. 6, in the present study. By this suggestion, determined results and effective check

relative parameters are given in Table 3. From the data, the specimen scales have few of differences to measure directly the fracture roughness K_{IQ} values in plan strain state. This indicates the moderate reasonability of the present suggestion and, when the crack growth increments are scattered significantly, the code-based measurement for ductile fracture roughness may be failure, appropriate measurement should be taking the 90 % J_{Imax}.

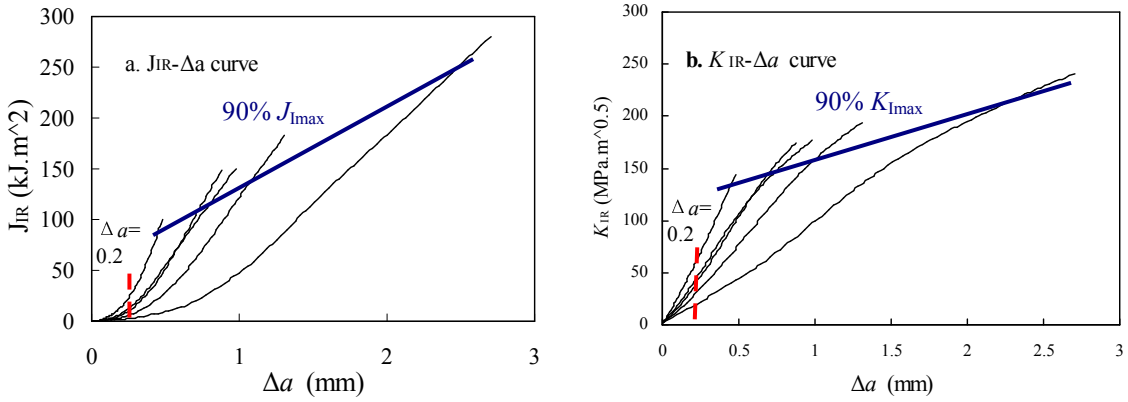

Fig. 5 Measurement scheme of fracture roughness values for the present material.

Table 3 Results by the suggestion of 90 % J_{Imax} for ductile fracture roughness measurements.

Specimen	a_o/W	W/B	W-a_o (mm)	Δa (mm)	J_{IQ} (kJ.m^{-2})	J_{Imax} (kJ.m^{-2})	K_{IQ} (MPa.m$^{-0.5}$)	K_{Imax} (MPa.m$^{-0.5}$)	$0.4(k_{IQ}/\sigma_Y)^2$ (mm)
1	0.5992	2.2093	44.35	0.88	57.8226	148.0125	108.2647	174.816	38.23
2	0.6063	2.2118	43.54	2.90	66.4216	108.9796	117.4546	150.004	43.91
3	0.6159	2.1920	42.15	0.48	72.8635	98.3216	108.3277	143.203	37.58
4	0.6099	2.1994	42.98	0.98	60.7256	150.6044	111.9739	176.340	40.15
5	0.6001	2.2104	44.23	2.70	60.7680	280.5483	111.9941	240.677	40.18

Probabilistic Measurement. For the determined K_{IQ} data in Table 3, an appropriate statistical distribution, lognormal distribution, is determined through comparing the total fit effects, consistency between failure physics and predictions, and safety prediction in tail region, similar to the determination of appropriate model for fatigue lives [17]. The fracture roughness, $K_{IC,P\text{-}C}$, at arbitrary *P-C* levels can be evaluated using formula

$$K_{IC,P-C} = 10^{(\lg K_{Ic})_{av}-[Z_P+t_{1-C}(n_s-1)](\lg K_{Ic})_{rms}} \tag{3}$$

where $\lg K_{IC,av}$ and $\lg K_{IC,rms}$ are average value and standard deviation of the test logarithms of fracture roughness K_{ICi} data; i=1, 2, …, n_s; n_s is number of the K_{IC} data. For the present tests, $\lg K_{IC,av}$, $\lg K_{IC,rms}$ and n_s are 2.04828, 0.0166754, and 5. Statistical curves for failure rate, probability density function, and cumulative distribution function are exhibited in Fig. 6. Probabilistic values for the K_{IC} measurements at specified *P-C* values are given in Table 4.

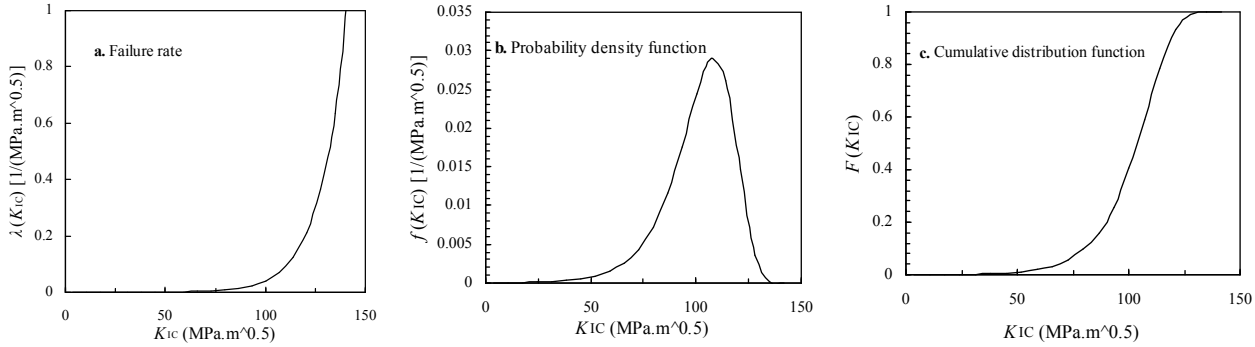

Fig. 6 Statistical curves of the fracture roughness values for the present material.

Table 4 Measurements for fracture roughness values at specified *P*-*C* levels.

C (%)	*P*	K_{IC}	*C* (%)	*P*	K_{IC}
50	0.5	111.758	95	0.5	102.975
	0.9	106.392		0.9	98.0303
	0.95	104.918		0.95	96.6723
	0.99	102.209		0.99	94.1755
	0.999	98.2542		0.999	91.4534
	0.9999	96.8868		0.9999	88.2720
90	0.5	105.369	99	0.5	96.7828
	0.9	100.310		0.9	92.1357
	0.95	98.9201		0.95	90.8593
	0.99	96.3652		0.99	88.5127
	0.999	93.5798		0.999	85.9542
	0.9999	91.3477		0.9999	83.9040

Summary

Due to be limited by production structural geometry, a ductile fracture roughness measuring method is employed, i.e. the ductile resistance J_{IR} curves should be determined firstly and the fracture resistance K_{IR} curve in plan strain state should be obtained through a converting formula.

When crack growth increments are very scattered, the measurement of 0.2 mm crack growth increment for gauge ductile fracture roughness, J_{IC}, may not reasonable. 90 % maximum ductile fracture roughness, J_{Imax}, should be suggested as an appropriate measurement.

New suggested 90 % J_{Imax} measurement is verified to be appropriate for measuring the ductile fracture roughness values of the present material.

Acknowledgement

The present research is supported by Natural Science Foundation of China (50821063 and 50575189), and Railway Science and Technology Research and Development Program (2004J013).

References

[1] B.H. Park and K.Y. Lee: Proc. Inst. Mech. Engrs, Part F: J. Rail and Rapid Transit Vol. 220 (2006), p. 201
[2] B.H. Park, N.P. Kim, J.S. Kim and K.Y. Lee: Vehicle. Syst. Dyn. Vol. 44 (2006), p. 887
[3] A.M. Pye: Materials and Design Vol. 3 (1982), p. 534
[4] P.E. West: Computer-Aided Design Vol. 1 (1969), p. 25
[5] M.G.D.V. Cuppari, F. Wischnowski, D.K. Tanaka and A. Sinatora: Wear Vol. 225–229 (1999), p. 517
[6] L. Cao and G.Y. Zhou: Materials Characterization Vol. 36 (1996), p. 65.
[7] Y.X. Li and X. Chen: Materials Science and Engineering A Vol. 308 (2001), p. 277
[8] T. Branza, F. Deschaux-Beaume, G. Sierra and P. Loursa: J. Mater. Proc. Tech. Vol. 209 (2009), p. 536
[9] J.C. Gregory: wear, fretting and fatigue. Wear Vol. 9 (1966), p. 249
[10] Z. Colburn: J. Franklin Inst. Vol. 80 (1865), p. 41
[11] M.S. Mikhalev, E.A. Muravev, L.I. Bershtein and L.P. Zhitova: Strength Mater. Vol. 13 (1981), p. 1434
[12] J. Kim and H.Y. Jeong: Int. J. Fatigue Vol. 32 (2010), p. 1159
[13] V.B. Tskipurishvili: Welding Int. Vol. 7 (1993), p. 308
[14] W.B. Adams: J. Franklin Inst. Vol. 79 (1865), p. 217
[15] S. Kinnersley and A. Roelen: Safety Science Vol. 45 (2007), p. 31
[16] Y.X. Zhao and B. Yang: Adv. Mater. Res. Vol. 118-120 (2010), p. 90
[17] Y.X. Zhao, Q. Gao and J.N. Wang: Reliab. Eng. Sys. Saf. Vol. 67 (2000), p. 1